Influence of Fine Particle Bombarding on Surface Strength of Carburized Steel under Rolling Contact Condition

Yuji Ohue 1 and Yuji Senno 2

1 Kagawa University, 2210-1, Hayashi-cho, Takamatsu-shi, Kagawa 761-0396, Japan
2 Yuasa, Co. Ltd., 6, Kume, Okayama-shi, Okayama, 701-0144, Japan

ABSTRACT

In order to evaluate the influence of fine particle bombarding (FPB) process on the surface strength of the carburized steel, four kinds of test specimens, which are as-carburized, ground and FPBed ones, were fatigue tested using a ball-on-disk type testing machine under a constant loading, The results of the fatigue tests were discussed using the statistic analysis and the observations on the surface properties after the fatigue tests. From the test results, there was a good possibility that the FPB process after carburizing will be available for the purpose to increase the fatigue life by the improvement of the abnormal layer. The formation of the wear trace of the FPBed disk during the fatigue process was different from that of the as-carburized and ground disks and the FPB process might control the propagation of the fatigue crack due to flaking.

Key Words: Rolling Fatigue Strength, Fine Particle Bombarding, Carburizing, Abnormal Layer, Weibull Distribution

1. Introduction

Generally, sliding-rolling contact machine elements have been surface-hardened by several heat treatments to increase surface durability and wear resistance as shown in Fig. 1. In many cases, gas-carburizing has been used for the heat treatment. The gas-carburizing produces the abnormal layer, which is oxidized and nonmartensitic, near the surface of the elements and causes the deterioration of the accuracy of the elements (Suzuki, 1998), (Yoshizaki, 1999). In order to remove the abnormal layer and to improve the accuracy, grinding process has been adopted after carburizing in the conventional process. However, it takes for hours to grind the surface. In this paper, fine particle bombarding process was substituted for the grinding one to decrease the time of the final finishing and to improve the carburized surface layer.

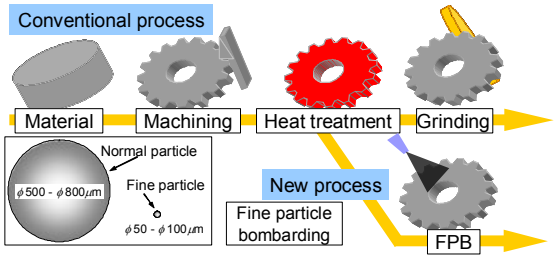

Fig.1 Application of FPB to surface finishing

The fine particles which have a diameter of 50μm to 100 μm were used for the fine particle bombarding (FPB). Normally, the FPB has the good advantage on the processing time, since the FPB processing time is shorter than the grinding one. Furthermore, the bombarding process with the fine particles provides the smaller surface roughness compared with the normal particles (Kagaya, 2006). When the FPB process is employed for the final finishing after carburizing, it is important to investigate the surface strength under a rolling contact condition. Therefore, four kinds of test

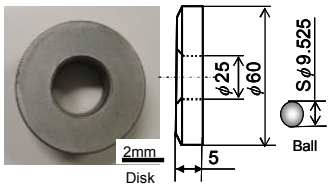

Material	C	Si	Mn	P	S	Ni	Cr	Mo	Cu	Fe
SCM420H	0.21	0.25	0.84	0.02	0.03	0.03	1.00	0.15	0.02	Bal.
SUJ2	1.00	0.25	0.30	0.02	0.01	1.40				Bal.

(wt%)

Fig.2 Shapes, dimensions and chemical compositions of test specimens

Table 1 Characteristics of test disks

Specimen		As-C	GC	AM50	AM100
Material		SCM420H			
Pre-machining		Grinding			
Heat treatment		Carburizing			
Surface finishing		---	Grinding*	FPB	
FPB particle	Material	---	---	Amorphous alloy	
	Size μm	---	---	50	100
	Hardness HV	---	---	900-950	
Surface hardness HV		619	783	855	929
Surface roughness	Ry μm	5.8	2.5	2.6	3.8
	Ra μm	0.49	0.21	0.33	0.42

*Specimen GC was ground up to 50μm from the surface after carburizing.

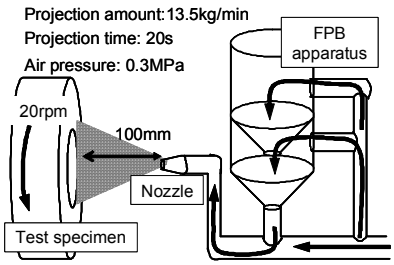

Fig.3 Conditions of FPB process

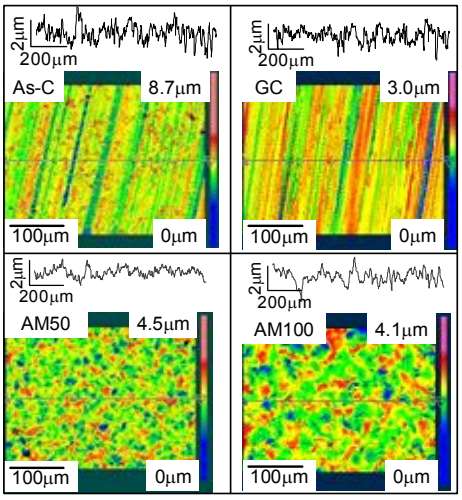

Fig.4 Surface profiles and topographys

specimens, which are as-carburized, ground and FPBed ones, were fatigue tested using a ball-on-disk type testing machine under a constant loading. The results of the fatigue tests were discussed using the statistic analysis and the observations on the surface properties after the fatigue tests.

2. Experimental Procedure of Fatigue Test

2.1. Test specimen Fig. 2 shows the shapes, the dimensions and the chemical compositions of the test specimens. The disk which has an outer diameter of 60mm and a thickness of 5mm was made from JIS SCM420H steel. The ball with a diameter of 9.525mm (3/8 inches) was made from JIS SUJ2 steel. Table 1 shows the characteristics of four kinds of test disks. Four kinds of test disks were carburized. One (As-C) of them was as-carburized. The specimen mark GC indicates that the disk was ground up to 50μm from the surface after carburizing to remove the abnormal layer due to carburizing. The specimen marks AM50 and AM100 indicates that the disks were fine-particle-bombarded using fine particles with a mean diameter of 50μm and 100 μm after carburizing, respectively. The sketch of the apparatus of fine particle bombarding (FPB) is shown in Fig. 3. The FPB process was carried out by mixing the compressed air with the fine particles.

The surface profiles obtained by a contact stylus instrument and the surface topography obtained by an instrument using the interferometric method are shown in Fig. 4. From the observation of the surface topography, the traces due to grinding existed in the cases of test disks As-C and GC, while the traces like dimples existed in the cases of the test disks AM50 and AM100. The size of dimples of the test disk AM50 was smaller than that of the test disk AM100. The ball was heat-treated by quenching and tempering. The surface roughness and the hardness of the ball were 0.004μmRa and HRC64 (HV800), respectively.

2.2. Fatigue test Fig. 5 shows the testing machine used for the rolling contact fatigue test. The testing machine is a ball-on-disk type. The fixed test disk was set with balls supported by a retainer and a race in the chamber. In this paper, three balls were come into contact with the fixed test disk. The applied normal load P a ball is 2128N, therefore, the load P yields the maximum Hertzian contact stress $p_{\max}$=6.15GPa (Johnson, 1999). The turbine oil was employed for the lubricant. The rolling contact fatigue test was conducted under a rotational speed of the shaft connected with the balls of 1700rpm at the room temperature (293K-303K). The balls revolve at a speed of 3.47m/s. The vibration sensor was installed on the lever for loading to detect the failure of the disk. The fatigue life of the disk was defined as the number of contact cycles between the disk and three balls, when the testing machine was automatically stopped owing to the increase in the vibration of the testing machine caused by the failure of the disk. The minimum oil film thickness was 0.197μm in this test condition, according to the reference (Hamrock, 1981). After the fatigue tests, the profile of the wear traces of the disks was measured using a contact stylus instrument and the surface was observed by an optical microscope. Then, the residual stress was measured using X-ray diffraction.

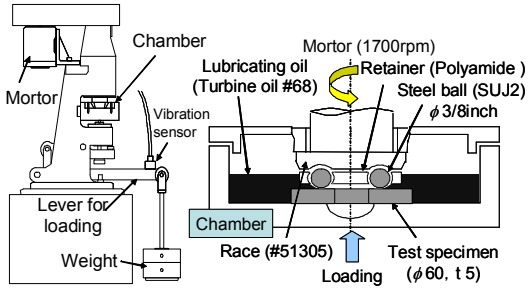

Fig.5 Testing machine for fatigue test

3. Rolling Fatigue Test Results and Discussions

3.1. Evaluation by Weibull plot and nonparameteric test Fig. 6 shows the 3-parameter Weibull plots of the fatigue lives N of test disks under the maximum Hertzian contact stress $p_{\max}$=6.15GPa. Furthermore, the mean fatigue life N_{m} of each disk is shown. The mean fatigue lives of both the test disks AM50 and AM100 were longer than that of the test disk As-C. As the cumulative probability became higher, the lives of both the test disks AM50 and AM100 were longer remarkably than that of the test disk As-C. In the case of the test disk GC, the lives varied widely compared with the others.

The nonparametric method, which is Wilcoxon signed-rank test, was calculated under two-sided test to check the significant difference among the fatigue lives of the test disks, since the number of tested specimens for each disk was less than 10 in this paper. In this case, the alternative hypothesis H_1 is “Disk A is different from disk B in the fatigue life.”, therefore, the null hypothesis H_0 is “Disk A is not different from disk B in the fatigue life.”. Table 2 shows the results

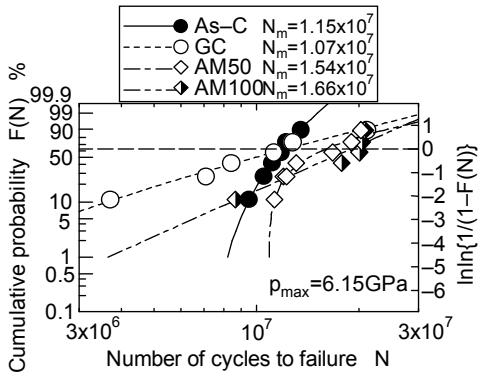

Fig.6 Weibull plots of rolling fatigue tests

Table 2 Results of nonparametric tests

	As-C	GC	AM50	AM100
As-C		× U=0.640513	○ U=-2.08167	× U=-1.60128
GC	× U=-0.64051		× U=-1.60128	× U=-1.4415
AM50	○ U=2.08167	× U=1.60128		× U=-0.64051
AM100	× U=1.60128	× U=1.4415	× U=0.640513	

Table 3 Rejection regions on H_0

	As-C	GC	AM50	AM100
As-C		52.20%	3.80%	11.00%
GC	52.20%		11.00%	15.00%
AM50	3.80%	11.00%		52.20%
AM100	11.00%	15.00%	52.20%	

of Wilcoxon signed-rank tests under a level of significance of 5%. In the only case of comparison of the test disk As-C with the test disk AM50, the null hypothesis was rejected, that is, the test disk AM50 was different from the test disk As-C in the fatigue life. However, as the level of significance was loosened, the nonparametric evaluations indicated that the FPBed disks AM50 and AM100 are different from the disks As-C or GC in the fatigue life at a level of significance 15% or less, as shown in Table 3. The fatigue lives of the test disks varied widely, since grinding in the amount of 50μm from the surface might incompletely remove the abnormal layer.

3.2. Surface properties after fatigue test Fig. 7 shows the failed surfaces, the wear traces and those profiles after the fatigue tests. The failure mode of all test disks was flaking caused by subsurface cracking. The profiles of the wear traces along white dotted lines were characterized by the parameters as shown in Fig. 8. The parameters w_d and w_z are the width and the depth of the wear trace, respectively. In Fig. 8, the relationships between those parameters and the fatigue lives N are shown. The width w_d was about 1mm and was larger than the diameter of the Hertzian contact area. The range of the depth w_z was about from 10μm to 20μm.

Fig. 9 shows the radius R_w of curvature of the wear trace and the maximum contact stress p_{max} based on the obtained radius of wear trace against the fatigue life N. The radius R_w was approximated from the profile of the wear trace by circular fitting. The stress p_{max} after the fatigue test was calculated from a ditch shape with the radius R_w of curvature of the wear trace in contact with the ball, which has a radius of 4.763mm. The R_w ranged about from 8mm to 14mm. Therefore, the p_{max} at the fatigue life which became a range of about 5.5GPa to 4.5GPa was less than the contact stress of 6.15GPa before the fatigue test.

Fig. 10 shows the residual stresses $(\sigma_r)_r$ and $(\sigma_r)_c$ before and after a fatigue test. The radial residual stress $(\sigma_r)_r$ and the circumferential stress $(\sigma_r)_c$ after the fatigue test was measured on the wear trace. In the cases of test disks AM50 and AM100, the stresses $(\sigma_r)_r$ and $(\sigma_r)_c$ were compressive before the fatigue tests. The compressive values of the stresses decreased after the fatigue tests. While, in the cases of test disks As-C and GC, the stresses $(\sigma_r)_r$ and $(\sigma_r)_c$ were about zero or slightly tensile before the fatigue tests. After the fatigue tests, the tensile stresses became almost the same compressive values as FPBed disks.

From the above discussions, the profile of the wear

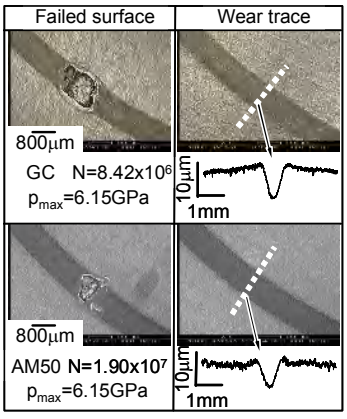

Fig.7 Failed surface and wear trace

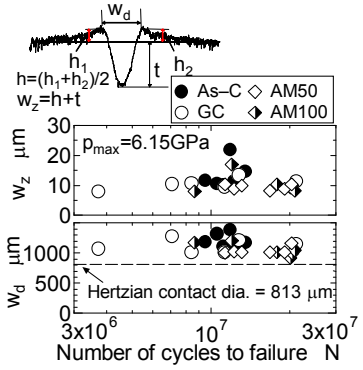

Fig.8 Relationship between parameters of wear trace and fatigue life

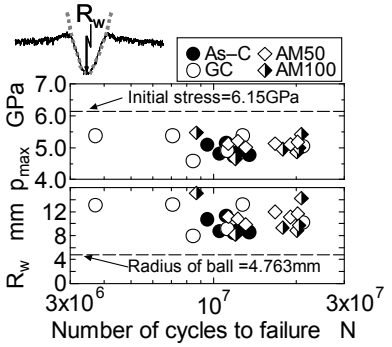

Fig.9 Radius curvature and contact stress against fatigue life

trace at the final fatigue stage did not depend on the surface finishing and the fatigue life. However, during the fatigue process, the change in the residual stress of FPBed test disks was different from that of test disks As-C and GC. This evidence shows that the formation of the wear trace of the FPBed disk during fatigue process is different from that of the as-carburized and ground disks.

3.3. Failure depth of flaking In order to discuss the depth of flaking using the internal stress distribution and the profile of the wear trace after the fatigue test, the internal stress was calculated by the finite element analysis. As shown in Fig. 9, the radius R_w of curvature of the wear trace was in the range of about from 8mm to 14mm. Therefore, the FEM analysis for calculating the internal stress was conducted under three cases of the ditch shapes with $R_w = \infty$, 8mm and 14mm in contact with the ball having a radius of 4.763mm. Fig. 11 shows the maximum shear stress τ_{max} and von Mises stress σ_e along z axis, which are the fracture criteria. The stresses below the surface along z axis became smaller, as the radius R_w became smaller. In spite of the radius R_w, the depths where the stresses indicated the maximum values were almost the same. The depth was about 0.2mm. Namely, the radius of curvature of the wear trace does not influence the depth where the stresses τ_{max} and σ_e became the maximum values. The wear depth as shown in Fig. 8 was less than about 20μm. In this fatigue test, therefore, the failure depth of the flaking can be evaluated using the internal stress distribution in the case of the contact between the ball and the flat disk.

Fig. 12 shows the failure depths of the flaking for each test disk against the fatigue life. The depth of the flaking was measured by a microscope with the function to measure the focal distance from the object. The depth ranged in about from 0.1mm to 0.2mm, which was shallower than the depth at the maximum value of the maximum shear stress τ_{max} in spite of the test disks.

3.4. Oil film thickness In order to discuss the influence of FPB on the lubricating condition, the oil film thickness was calculated using a commercial software TED/CPA based on the Reynolds equation according to elast-hydro dynamic (EHL) theory (Hamrock, 1981). Fig. 13 shows the models for calculating. Four kinds of models were prepared. Model 1 and Model 2 are employed for the smooth disk surface and the worn one, respectively. Model 3 and Model 4 are employed for the FPBed disk surface and the ground one, respectively. Figs. 14 and 15 show that the oil film thickness h and the EHL pressure distributions along the moving direction of the ball, respectively. At the initial fatigue stage, it was estimated that the thickness h on the FPBed disks was the thickest in all test disks. While, the EHL pressure on the FPBed disks indicated the highest value. The lubricating condition on the FPBed disk at the initial fatigue stage was not always superior

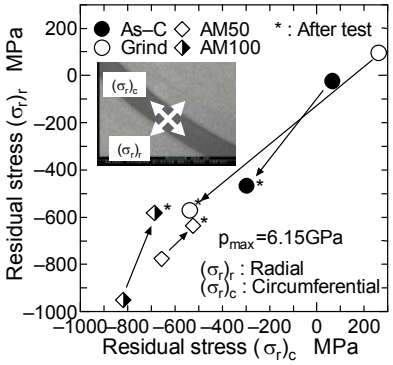

Fig.10 Residual stresses of surface before and after fatigue test

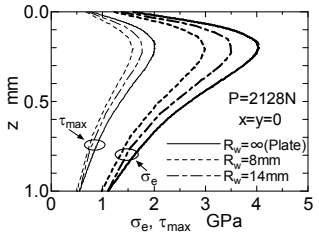

Fig. 11 Internal stresses below surface

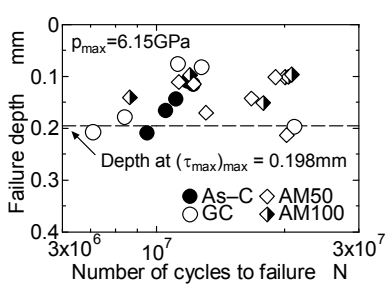

Fig. 12 Failure depth of flaking

to the others in this contact condition, taking the above EHL analysis into account. At the final fatigue stage, the thickness and the pressure on the worn surface of all test disks became thicker and lower compared with those at the initial fatigue stage, respectively.

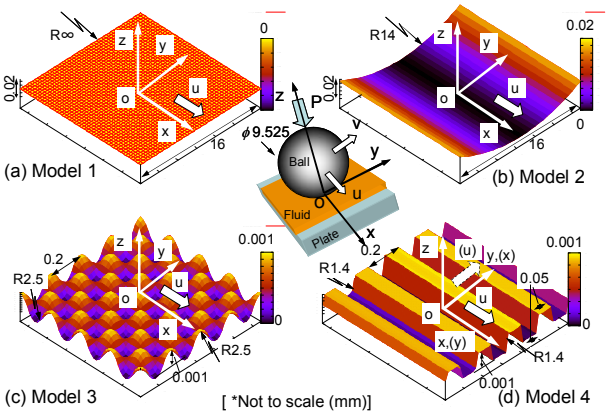

Fig.13 Models for calculating lubricating condition

4. Conclusions

The following can be concluded from the fatigue tests and the discussions.

(1) From the observation of the surface topography, the traces due to grinding existed in the cases of as-carburized and ground disks, while the traces like dimples existed in the cases of the FPBed disks.

(2) From the results of both the Weibull plot and the nonparametric test, there was a good possibility that the FPB process after carburizing will be available for the purpose to increase the fatigue life by the improvement of the abnormal layer.

(3) The formation of the wear trace of the FPBed disk during fatigue process is different from that of the as-carburized and ground disks. The FPB process might control the propagation of the fatigue crack due to flaking. therefore, the FPBed disks had longer fatigue life.

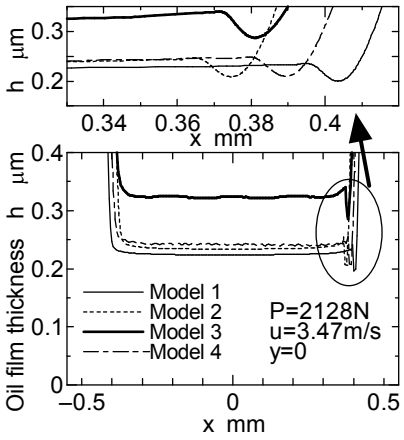

Fig.14 Oil film thickness

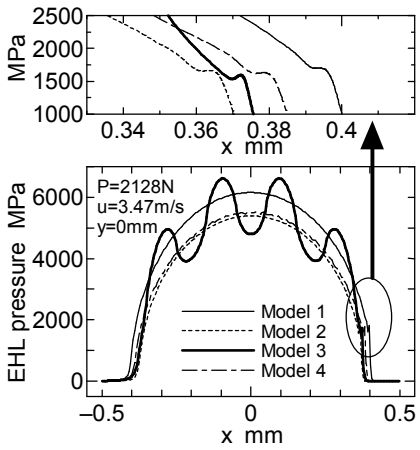

Fig.15 EHL contact pressure

Acknowledgment

This research was financially supported by JSPS Grants-in-Aid for Scientific Research and JST Innovation Satellite Tokushima. The FPB process and the surface measurements were carried out in cooperation with Sintokogio, Ltd. and Amatsuji Steel Ball Mfg. Co., Ltd., respectively. The authors deeply appreciate their cooperation.

References Hamrock, B. J. and Dowson, D., "Ball Bearing Lubrication", John Wiley & Sons, 1981.

Johnson, K. L., "Contact Mechanics", Cambridge Univ. Press, 1999.

Kagaya, C., "Development Trends and Technical Outlooks of Fine Particle Peening (FPB)", Journal of JSPE, Vol. 72, No. 9, 2006, 1097-1070 (In Japanese).

Suzuki, T., Ogawa, K. and Hotta, S., "Influence of Oxidized and Nonmartensitic Layer, and Surface Roughness on Pitting Fatigue Strength of Carburized Steel", Transactions of JSME, Series C, Vol. 64, No. 622, 1998, 2199-2204 (In Japanese).

Yoshizaki, M. and Hashimoto, "Effect of Abnormal Surface Layer on Tooth Surface Strength of Gas Carburized Gear", JSME, Series C, Vol. 65, No. 630, 1999, 694-701 (In Japanese).